

Optimized Structures of Bimetallic Systems: A Comparison of Full- and Broken-Symmetry Density Functional Calculations

Timothy Lovell,[†] John E. McGrady,[†] Robert Stranger,^{*,†} and Stuart A. Macgregor[‡]

Department of Chemistry, Faculties, and Research School of Chemistry, The Australian National University, Canberra, ACT 0200, Australia

Received December 7, 1995

The electronic structure of complexes containing multiple metal–metal bonds remains a topic of enduring interest to coordination chemists.¹ Among bimetallic systems, the family of face-shared bioctahedral complexes, M_2X_9 , present a unique opportunity to study periodic trends in metal–metal interactions due to their widespread occurrence throughout the first, second, and third transition series.² The structural characteristics of complexes of the series $M_2Cl_9^{3-}$, $M = Cr, Mo, W$, exemplify the trends in metal–metal bonding down a triad. Despite the formal bond order of 3 in each case, metal–metal separations change dramatically within the triad, decreasing from approximately 3.10 Å for the chromium complex³ to 2.45 Å for its tungsten analogue.⁴ Mo–Mo separations lie between these two extremes, and are also notably cation dependent, spanning a range of values from 2.52 to 2.78 Å.⁵

Quantitative information regarding the metal–metal bonding has been considerably more difficult to obtain, principally due to the well-documented limitations of molecular orbital theory in describing weakly coupled electrons.⁶ The imposition of full molecular symmetry (in this case D_{3h}) leads to a complete delocalization of the magnetic orbitals over both centers, a result which is clearly physically unrealistic in the limit of weak electronic coupling or infinitely large metal–metal separations. The broken-symmetry technique developed by Noodleman⁷ represents a significant step forward in this respect. By removing those symmetry elements relating the halves of the dimer and introducing asymmetry in the spin density at the two metal centers, it is possible to treat the two ions as distinct, weakly interacting units, thereby permitting the magnetic electrons to localize on one center or the other.

The broken-symmetry approach has been employed with considerable success to interpret the magnetic and spectroscopic properties of a variety of biologically significant species.⁸ The widespread application of the method has however been limited by availability of accurate structural data. Crystallographically characterized species form only a small subset of the series of

known binuclear complexes, and there is currently much interest in describing the electronic structure of unstable oxidation states⁹ for which structural data are less common.

The influence of symmetry breaking on the molecular structure, particularly the metal–metal separation, in polynuclear transition metal complexes has received less attention. A number of papers have reported manual optimizations on naked metal dimers, notably Cr_2 and Mo_2 ¹⁰ using broken-symmetry wave functions, while Ziegler and co-workers have optimized metal–metal bond lengths in a variety of unsupported metal dimers.^{10e,11} The majority of dimeric metal complexes of relevance to both inorganic and bioinorganic chemistry feature a variety of bridging ligands, which present additional complexity over and above that of unsupported dimers, due to the complex interplay of metal–metal and metal–bridge interactions. In recent years, gradient techniques for geometry optimization¹² have been incorporated into density functional codes. It is of considerable interest to see whether these automated optimization routines, in conjunction with broken-symmetry wave functions, provide improved estimates of metal–metal separations in bridged bimetallic systems in comparison to calculations performed using the full molecular symmetry. We note at this point that the broken-symmetry state does not correspond to a pure spin state, and therefore, optimized geometries do not necessarily correspond to those of the true ground state. However, in a recent study on Cr_2 ,^{10d} Becke and co-workers minimized the energy of both the broken-symmetry state and the true ground state, the latter being obtained by approximate spin projection techniques. With the majority of density functionals, a close correspondence between Cr–Cr bond lengths was found for the broken-symmetry and true ground states. It is not possible to incorporate spin projection into the automated geometry optimization procedure, but we anticipate that, in the more complex systems described here, the broken-symmetry minimum will also correspond closely to that of the true ground state.

In this communication, we report preliminary results of geometry optimizations on the nonchlorides of the chromium

[†] Department of Chemistry.

[‡] Research School of Chemistry.

- (1) Cotton, F. A.; Walton, R. A. *Multiple Bonds Between Metal Atoms*; Oxford University Press: Oxford, U.K., 1993; see also references therein.
- (2) (a) Summerville, R. H.; Hoffmann, R. *J. Am. Chem. Soc.* **1979**, *101*, 3821. (b) Ginsberg, A. P. *J. Am. Chem. Soc.* **1980**, *102*, 111. (c) Cotton, F. A.; Ucko, D. A. *Inorg. Chim. Acta* **1972**, *6*, 161. (d) Stranger, R. *Inorg. Chem.* **1990**, *29*, 5231. (e) Heath, G. A.; McGrady, J. E. *J. Chem. Soc., Dalton Trans.* **1994**, 3767. (f) Gheller, S. F.; Heath, G. A.; Humphrey, D. G.; Hockless, D. C. R.; McGrady, J. E. *Inorg. Chem.* **1994**, *33*, 3986.
- (3) (a) Saillant, R.; Wentworth, R. A. D. *Inorg. Chem.* **1968**, *7*, 1606. (b) Wessel, G. J.; Ijdo, D. J. W. *Acta Crystallogr.* **1957**, *10*, 466. (c) Grey, I. E.; Smith, P. W. *Aust. J. Chem.* **1971**, *24*, 73.
- (4) (a) Dunbar, K. R.; Pence, L. E. *Acta Crystallogr.* **1991**, *C47*, 23. (b) Watson, W. H., Jr.; Waser, J. *Acta Crystallogr.* **1958**, *11*, 689. (c) Stranger, R.; Grey, I. E.; Madsen, I. C.; Smith, P. W. *J. Solid. State Chem.* **1987**, *69*, 162.
- (5) Stranger, R.; Smith, P. W.; Grey, I. E. *Inorg. Chem.* **1989**, *28*, 1271.
- (6) (a) Hopkins, M. D.; Gray, H. B.; Miskowski, V. M. *Polyhedron* **1987**, *6*, 705. (b) Hall, M. B. *Polyhedron* **1987**, *6*, 679.
- (7) Noodleman, L.; Norman, J. G., Jr. *J. Chem. Phys.* **1979**, *70*, 4903.
- (8) (a) Bencini, A.; Gatteschi, D. *J. Am. Chem. Soc.* **1986**, *108*, 5763. (b) Aizman, A.; Case, D. A. *J. Am. Chem. Soc.* **1982**, *104*, 3269. (c) Ross, P. K.; Solomon, E. I. *J. Am. Chem. Soc.* **1991**, *113*, 3246. (d) Noodleman, L.; Case, D. A. *Adv. Inorg. Chem.* **1992**, *38*, 423. (e) Medley, G. A.; Stranger, R. *Inorg. Chem.* **1994**, *33*, 3976. (f) Moussea, J.-M.; Chen, J. L.; Noodleman, L.; Bashford, D.; Case, D. A. *J. Am. Chem. Soc.* **1994**, *116*, 11898. (g) Brown, C. A.; Remar, G. J.; Musselman, R. L.; Solomon, E. I. *Inorg. Chem.* **1995**, *34*, 688. (h) Noodleman, L.; Baerends, E. J. *J. Am. Chem. Soc.* **1984**, *106*, 2316.
- (9) (a) Heath, G. A.; Raptis, R. G. *Inorg. Chem.* **1991**, *30*, 4107. (b) Heath, G. A.; Humphrey, D. G. *J. Chem. Soc., Chem. Commun.* **1990**, 672. (c) Kennedy, B. J.; Heath, G. A.; Khoo, T. J. *Inorg. Chim. Acta*, **1991**, *190*, 265.
- (10) (a) Delley, B.; Freeman, A. J.; Ellis, D. E. *Phys. Rev. Lett.* **1985**, *54*, 661. (b) Baykara, N. A.; McMaster, B. N.; Salahub, D. R. *Mol. Phys.* **1984**, *52*, 891. (c) Dunlap, B. I. *Phys. Rev. A* **1983**, *27*, 2217. (d) Edgecombe, K. E.; Becke, A. D. *Chem. Phys. Lett.* **1995**, *244*, 427. (e) Ziegler, T.; Tschinke, V.; Becke, A. D. *Polyhedron* **1987**, *6*, 685.
- (11) Ziegler, T. *J. Am. Chem. Soc.* **1985**, *107*, 4453.
- (12) (a) Versluis, L.; Ziegler, T. *J. Chem. Phys.* **1988**, *88*, 322. (b) Ziegler, T. *Chem. Rev.* **1991**, *91*, 651.

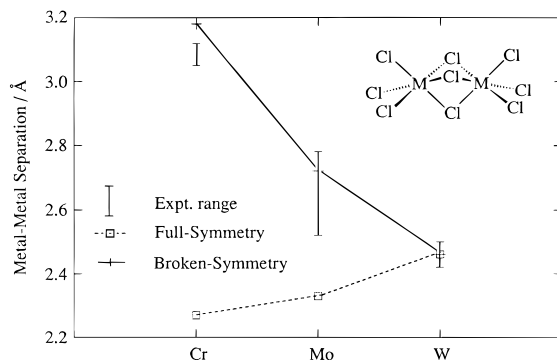


Figure 1. Comparison of optimized and experimentally determined metal–metal separations in $M_2Cl_9^{3-}$, $M = Cr, Mo, W$.

triad, $Cr_2Cl_9^{3-}$, $Mo_2Cl_9^{3-}$ and $W_2Cl_9^{3-}$. All independent structural parameters were optimized using both conventional molecular orbital (D_{3h} symmetry) and broken-symmetry (C_{3v} symmetry) techniques.¹³ Optimized metal–metal separations for $Cr_2Cl_9^{3-}$, $Mo_2Cl_9^{3-}$ and $W_2Cl_9^{3-}$ are summarized in Figure 1, along with the available crystallographic data. It is immediately apparent that while broken-symmetry calculations accurately reproduce the experimental trend toward shorter M–M separations in the heavier congeners, the imposition of full-symmetry results in the completely opposite trend. For the chromium complex, the full-symmetry calculation severely underestimates the metal–metal separation, the optimized value lying 0.9 Å below the crystallographically determined range (3.05–3.12 Å).³ In contrast, the optimized broken-symmetry structure has a Cr–Cr distance only approximately 0.1 Å higher than the experimentally observed values. The broad spectrum of crystallographically determined Mo–Mo separations makes the absolute accuracy of the different methods difficult to assess. It is, however, clear that while the full-symmetry estimate is 0.2 Å lower than even the shortest experimentally determined value, the optimized distance of 2.71 Å obtained from broken-symmetry calculations lies in the center of the experimental range.⁵ In stark contrast to the case of complexes in the first and second transition series, identical W–W separations are obtained from both full- and broken-symmetry calculations, the optimized values being in excellent agreement with the available experimental data.⁴

To understand the electronic origin of these trends, we must consider the distribution of the magnetic orbitals involved in mediating the metal–metal interaction. As noted above, in the molecular orbital (full-symmetry) method, each magnetic orbital is constrained to have an equal amplitude on each of the two metal centers. In contrast, breaking the spatial symmetry allows the electrons to localize if such an arrangement is energetically favorable. Contour plots of the spin-up σ and δ_π ¹⁶ magnetic orbitals of $Cr_2Cl_9^{3-}$, $Mo_2Cl_9^{3-}$, and $W_2Cl_9^{3-}$ are shown in Figure

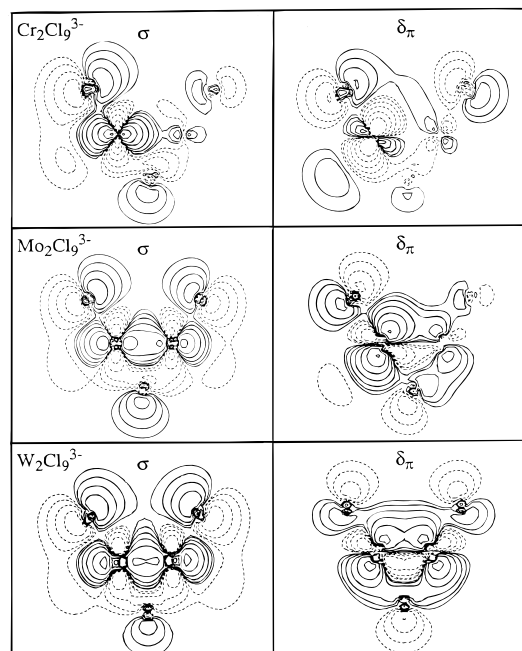


Figure 2. Broken-symmetry contour plots of the σ^\uparrow and δ_π^\uparrow magnetic orbitals of $Cr_2Cl_9^{3-}$, $Mo_2Cl_9^{3-}$, and $W_2Cl_9^{3-}$.

2, indicating that, on descending the triad, the magnetic electrons become progressively more delocalized. In light of the complete localization of both σ and δ_π electrons in $Cr_2Cl_9^{3-}$, it is not surprising that the full-symmetry solution provides such a poor estimate of the Cr–Cr separation. At the opposite extreme, the magnetic orbitals in $W_2Cl_9^{3-}$ are completely delocalized, and the full- and broken-symmetry approaches yield identical W–W separations. In $Mo_2Cl_9^{3-}$, the δ_π electrons remain trapped on one center, but there is considerable delocalization of the σ -electron density. The molybdenum system therefore represents an intermediate bonding situation, and accordingly, there is less disparity between full- and broken-symmetry results than for the chromium analogue, although the full-symmetry estimate is still unrealistically short.

In summary, a comparison of full- and broken-symmetry calculations indicates that where the overlap of magnetic orbitals is weak, the use of broken-symmetry is essential for a quantitatively correct description of the molecular geometry. Imposing complete delocalization of the metal-based electrons through use of conventional (full-symmetry) molecular orbital calculations results in unrealistically short metal–metal separations. Where the orbital overlap is relatively strong, as it clearly is in $W_2Cl_9^{3-}$, the molecular orbital and broken-symmetry methods converge to give identical predictions of the metal–metal separation. The accuracy of the broken-symmetry optimizations illustrated here indicates that this approach may be extremely useful as a predictive tool for experimentalists investigating highly reactive species for which conventional structural data are likely to remain elusive. We are currently assessing the utility of this method on a much broader range of bimetallic systems.

Acknowledgment. The financial support of the Australian Research Council to R.S. is gratefully acknowledged, as is the Engineering and Physical Sciences Research Council (U.K.) for provision of an overseas studentship to T.L.

IC951564K

(13) Spin-unrestricted calculations were performed within the local-density approximation,¹⁴ using the ADF package developed by Baerends and co-workers.¹⁵ A triple- ζ STO basis was used to describe the metal ions, while a double- ζ basis augmented by a single d polarization function was used for Cl. Geometries were optimized using the algorithm of Versluis and Ziegler.^{12a} In molecular orbital calculations, the full D_{3h} point symmetry of the molecule was utilized. In the broken-symmetry calculations, all symmetry elements connecting the two metal centers were removed, resulting in C_{3v} symmetry. Calculations were also performed with the addition of quasi-relativistic corrections, which were found to make only small changes to calculated M–M separations, even for $W_2Cl_9^{3-}$.

(14) Vosko, S. H.; Wilk, L.; Nusair, M. *Can. J. Phys.* **1980**, *58*, 1200.

(15) The Amsterdam Density Functional program. See: (a) Baerends, E. J.; Ros, P. *Int. J. Quantum Chem. Symp.* **1978**, *12*, 169. (b) Boerrigter, P. M.; te Velde, G.; Baerends, E. J. *Int. J. Quantum Chem. Symp.* **1988**, *33*, 307.

(16) In trigonal symmetry, the metal-based t_{2g} orbitals of an ideal octahedron are split into a single orbital of σ symmetry with respect to the metal–metal axis and a doubly degenerate pair with $2/3\delta$ and $1/3\pi$ character, denoted δ_π (see ref 2e for a detailed discussion).